



2. Magnon spectra in layered samples: From NN exchange to dipolar coupling

Jean-Claude Serge Levy

► To cite this version:

Jean-Claude Serge Levy. 2. Magnon spectra in layered samples: From NN exchange to dipolar coupling. Jean-Claude Serge Lévy. Nanostructures and their magnetic properties, S.G. Pandalai, pp.303-328, 2010, Research Signpost, 978-81-308-0371-5. hal-01166227

HAL Id: hal-01166227

<https://hal.science/hal-01166227>

Submitted on 22 Jun 2015

HAL is a multi-disciplinary open access archive for the deposit and dissemination of scientific research documents, whether they are published or not. The documents may come from teaching and research institutions in France or abroad, or from public or private research centers.

L'archive ouverte pluridisciplinaire **HAL**, est destinée au dépôt et à la diffusion de documents scientifiques de niveau recherche, publiés ou non, émanant des établissements d'enseignement et de recherche français ou étrangers, des laboratoires publics ou privés.



Research Signpost
37/661 (2), Fort P.O.
Trivandrum-695 023
Kerala, India

Nanostructures and their Magnetic Properties, 2009: ISBN: 978-81-308-0371-5
Editor: Jean-Claude Serge Lévy

12. Magnon spectra in layered samples: From NN exchange to dipolar coupling

Jean-Claude Serge Lévy

*Laboratoire MPQ, UMR7162 CNRS, 10 rue Alice Domon et Léonie Duquet
Université Paris 7, Denis Diderot, 75013 Paris, France*

Abstract. The dispersion relations of progressive spin waves and the stationary normal modes in thin films are derived according to a unified picture, by means of dynamical and transfer matrices. The full spectrum of stationary excitations and their localization properties are deduced. Numerical calculations confirm the increasing complexity of both dispersion relation and stationary mode localization when increasing interaction range. Recent experimental observations and micromagnetism simulations are confronted with these results.

PACS numbers: 75.30.Ds; 72.15.Rn

1. Introduction

Since the beginning of quantum mechanics applied to solid state physics [1], the magnetic excitations of a magnetic system have been studied and called spin waves or magnons [2] since they behave as standard elementary excitations, i.e. as bosons. Since magnetic stationary modes are submitted to strict boundary conditions which select them according to an effective Fabry-Perot

Correspondence/Reprint request: Dr. Jean-Claude Serge Lévy, Laboratoire MPQ, UMR7162 CNRS, 10 rue Alice Domon et Léonie Duquet, Université Paris 7, Denis Diderot, 75013 Paris, France.
E-mail: jean-claude.levy@univ-paris-diderot.fr

matching condition [3], stationary magnons have been early observed in magnetic thin films by means of spin wave resonance [4]. This condition well separates quite numerous resonance lines for a thin film.

Magnetic excitations strongly depend on the nature of the magnetic interactions which occur within the sample. For a Heisenberg magnet these interactions are: exchange, superexchange, anisotropy, dipole-dipole interaction and Zeeman effect [5]. Exchange is a short range interaction which is due to the overlap between electronic clouds of neighbouring sites as it appears in the Heitler-London study of the H_2 molecule [6]. This approach has been generalized to the chemical bond of molecules and solids. So exchange interaction just connects a few sites. Anisotropy is due to spin-orbit coupling which is a consequence of the relativistic electronic motion localized within ions and atoms [7]. So anisotropy is a quite local notion even if some authors introduced also the concept of anisotropy induced by neighbouring sites because of the usual interplay of exchange and anisotropy [8]. Superexchange occurs only in complex materials such as metal oxides or metal-metalloid compounds where the magnetic superexchange interaction between metal electrons occurs through the electronic cloud of a polarized oxygen ion or metalloid ion by means of two successive overlaps between metal electronic wave function and oxygen or metalloid electronic wave function. Thus superexchange interaction is swiftly more extended than pure exchange in this Heisenberg picture. Dipole- dipole interactions, also called dipolar interactions [9], are the standard long distance interactions between classical magnets, i.e. they have a long distance $1/r^3$ behaviour as a function of the distance r between the interacting sites, and they have also a complex geometrical scheme since they depend on the mutual spin orientations and on their angles with the connecting vector \vec{r} . According to these respective orientations, dipolar interactions lead to ferromagnetism or to antiferromagnetism. A remarkable property of dipolar interactions is an enormous frustration [10] since for any given spin circuit, numerous dipolar interactions are competing together. This leads to the well observed complex domain structure of magnets. Finally Zeeman effect couples each spin to the local magnetic field.

So the effect of the interaction range upon spin wave properties is not a new question. For instance the distinction between exchange modes and magnetostatic modes was quite early proposed [11]. But this question remains still open since it gives rise to a quite complex problem on both structural and dynamic properties. For instance, a few years ago, the structural richness of the competition between two sorts of short range interactions, i.e. frustration [10], concentrated a lot of interest on axial next

nearest neighbour Ising (ANNNI) model, with the evidence of quite numerous phase transitions [12]. Now it must be added that both the present abundance of magnetic materials and the recent progress in realistic miniaturization of nanomagnets [13] reactivate the interest in the competition between different interaction ranges [14]. And nanotechnology develops a new point which is the interplay between interaction range and sample size. This competition is responsible for an increase of the already rich structural complexity of these new materials since it brings a new complex magnetic surface tension term among the already numerous competing causes acting on magnetic structure and dynamics.

Before going to practical purposes, it must be added that several systems show a clear analogy with magnetic systems. This is obviously the case of elastic systems which are well known to have phonon excited states in close analogy with magnetic magnon excited states, as reported for instance in the case of solid systems with impurity [15]. Analogy means also difference and it must be said that magnons are mathematically simpler than phonons even if their conception seems somewhat less easy than that of sound excitations. This simplicity is due to the dimensionality two of spin excitations which are locally normal to the equilibrium spin configuration. Atomic motions have a dimensionality three which is responsible for the existence of both longitudinal and transverse acoustic waves. The dimension two of spin waves is just that of a complex number and so is easily introduced mathematically. Physically it just corresponds to the two circular states of polarization as it occurs for light. Another difficulty for phonons as compared to magnons is the abundance of magnetic and non-magnetic elastic interactions to be compared with the only magnetic interactions occurring for magnons. As a result magnons are often used as a model for further phonon studies [15].

Of course chains of electronic systems are also of interest and can be compared with magnons. An electronic case somewhat similar to the present case of magnetic competing interaction ranges is the t - t' - J model [16] which has been considered for the complex structure of new high T_C superconductors. In that case, different overlaps between electronic wavefunctions and their environment are introduced. Of course electronic approaches which are derived from tight-binding views are also close to the present approach of competing interaction ranges with a common picture based upon the dynamical matrix [17]. In that case the interaction range is due to electronic wavefunction overlap.

In the present case of magnetic systems, it is necessary to first recall the basic nature of magnetic interactions and their contribution to the basic spin equation of motion, as done in a first part. Then the study of ingoing spin waves in such materials leads to deduce the spin wave dispersion relation.

This dispersion relation is revealed to be quite sensitive to the interaction range of magnetic interactions, as shown in different specific cases. These different dispersion laws are reported in a second part. The specific study of stationary modes in thin films is achieved in different ways, involving more or less numerical computation in order to derive practical results. This is done both on the classical basis of the dynamical matrix and on the more recent view of transfer matrix [18] which is reminiscent of the theory of electronic propagation in circuits [19]. The transfer matrix has also its origin in the classical resolution of mechanical problems with coupled systems [20]. So the principles of determination of these modes are shown in a third part. Finally conclusive remarks are devoted to underline the main results here obtained and to compare them with the present experimental state of the art. Applications to phonons and to electronic states are also suggested.

2. Magnetic interactions and spin motion in a layered material

As said in the introduction, the different magnetic interactions between Heisenberg vector spins located on site I : \vec{S}_i and other spins and the environment are just recalled here [2, 5-7, 9]. There is first exchange interaction [6]:

$$H_{exc} = -\frac{1}{2} \sum J_{ij} \vec{S}_i * \vec{S}_j \quad (1)$$

Here coupled neighbouring sites i and j are close enough to produce a real electronic wavefunction overlap which is characterized by the exchange integral J_{ij} . A non zero value of the exchange integral is usually restricted to nearest neighbours i and j . And its value can vary with environment as considered for surface and interface problems [3, 21]. Then there is anisotropy interaction [7]:

$$H_{anis} = -\sum d_i \left(\vec{S}_i * \vec{e}_i \right)^2 \quad (2)$$

It is restricted to the spin site where the local easy axis has for unit vector \vec{e}_i . The intensity of this coupling is given by the anisotropy parameter d_i . The anisotropy parameter is usually considered as uniform in the sample but can be considered as non uniform for surface and interface problems [3, 21]. In

the case of quasicrystals where several environments must be considered [14], several values of the anisotropy parameter must be considered. Superexchange interaction writes [5]:

$$H_{exc} = -\frac{1}{2} \sum J'_{ij} \vec{S}_i * \vec{S}_j \quad (3)$$

Here coupled neighbouring sites i and j are close enough to produce a real electronic wavefunction overlap through a non magnetic ion k which is magnetically polarized by its neighbours. As a consequence the strength of this interaction is given by the superexchange parameter J'_{ij} .

Dipole-dipole interaction writes [9]:

$$H_d = \sum_{i \neq j} \frac{\vec{S}_i * \vec{S}_j}{r_{ij}^3} - 3 \sum_{i \neq j} \frac{(\vec{S}_i * \vec{r}_{ij})(\vec{S}_j * \vec{r}_{ij})}{r_{ij}^5} \quad (4)$$

Here all spins interact with all other spins with the same coupling constant omitted here.

And finally Zeeman interaction writes [9]:

$$H_Z = -g \sum_i \vec{S}_i * \vec{H}_i \quad (5)$$

This local interaction submits each spin to the local field \vec{H}_i . A coupling parameter g is introduced.

The spin equation of motion can be deduced either from a classical approach [4] or from a quantum approach with linearization [3, 8]. Such results are quite similar to those of the Landau- Lifshitz- Gilbert (LLG) precession equation without Gilbert damping. In our case Gilbert damping just introduces resonance linewidth and so could be introduced phenomenologically. In a largely extended layered material such as a thin film and in presence of a saturating external magnetic field, most of the spins in the same layer are parallel and experiment the same interactions. So the problem of spin motion reduces to a one dimensional problem characterized by the complex spin deviation u_n in the layer n . The equation of motion couples together several spin deviations u_n relative to different layers. In the literature there are numerous examples of convenient thin film orientations cut in crystalline lattices with evidence for coupling with one or several

neighbouring layers according to the specific considered case [22], even in the case of an exchange interaction restricted to nearest neighbours. Of course in the general case of long range interaction such as dipolar interaction, all layers are coupled together. This is a limiting case, often neglected. In the bulk, interaction parameters can be assumed to be the same everywhere, thus it is easy to derive the standard bulk equation of spin motion on the spin amplitude u_n on the layer n [23] with bulk parameters, after introducing an oscillatory time behaviour such as $\exp(iEt)$ where E is the spin wave energy or frequency. When classifying the coupling with other layers according to their distance from the layer reference, this equation of motion reads:

$$(a - E)u_n - b(u_{n+1} + u_{n-1}) - c(u_{n+2} + u_{n-2}) - d(u_{n+3} + u_{n-3}) + \dots = 0 \quad (6)$$

Here a is the effective intralayer coupling, b the coupling with the two nearest layers, c to the coupling with the two next nearest layers and so on with increasing alphabetic order and increasing distance to the reference layer. The symmetric coupling on both sides of the rotating spin layer has for consequence the symmetry between ingoing waves and outgoing waves. For some crystallographic lattices and cuts, all layers are not equivalent, several sorts of equivalent layers can be distinguished [22]. This introduces a set of distinct equations (6) which is not considered here. Of course near external surfaces, some neighbouring sites are missing, this is the general reason for surface tension, and so even if interaction parameters remain unchanged near external surfaces, equations of motion are modified close to external surfaces. We do not deal specifically with such surface problems here, however we will introduce later some ways which can be used for solving such problems.

3. Dispersion relation for ingoing spin waves

The dispersion relation between pulsation ϖ and wavevector k for ingoing spinwaves of spin amplitude $u_n = C \exp[ikna_0 - i\varpi t]$ on layer n where a_0 is the interlayer distance, is straightforwardly deduced from the expression of the equation of motion (6) for this wave. For such modes the equation of motion reads as a one dimensional dispersion relation $E(k)$ between the spin wave energy E or pulsation ϖ and wavevector k :

$$E = a - 2b \cos(ka_0) - 2c \cos(2ka_0) - 2d \cos(3ka_0) - 2e \cos(4ka_0) - \dots \quad (7)$$

In more sophisticated geometrical cases [22], this basic formula must be corrected since layers are not all equivalent but the final result keeps the same principle of a sum of contributions. From equation (7), it is clear that the nature of the dispersion relation strongly depends on the interaction range, as considered below.

- 3.a. For instance, for a very local coupling restricted to the layer as it occurs with anisotropy only ($b = c = d = \dots = 0$), there is no dispersion at all:

$$E = a \quad (8)$$

- 3.b. For a coupling restricted to the nearest layer and the layer itself, as usually assumed: $a \neq 0, b \neq 0, c = d = \dots = 0$, the usual monotonic sinelike dispersion relation is obtained [3, 4]:

$$E = a - 2b \cos(ka_0) \quad (9)$$

The result of this equation shown on Figure 1 introduces both the magnon bandwidth $2b$, observed experimentally from neutron scattering and the “atomic exchange constant” for long ranged spin waves ba_0^2 , deduced from spin wave resonance observations [3, 4].

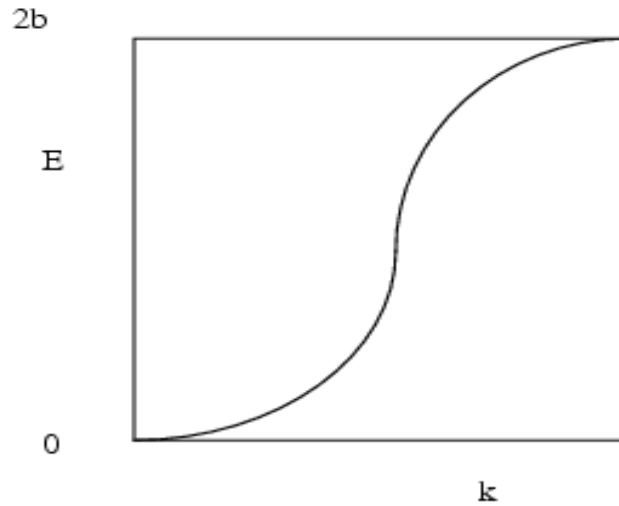


Figure 1. The spin wave spectrum for coupling restricted to the nearest layers ($a=0$). The magnon bandwidth is $2b$.

- 3.c For coupling with more than one pair of layers, ($a \neq 0, b \neq 0, c \neq 0, \dots$) a non monotonic dispersion law is easily obtained because of the cosine sum of equation (7). This is a quite general case! For instance, for a coupling restricted to two sorts of layers, the dispersion law for real wavevectors is non monotonic if $|c| > |b/4|$. That non monotonic behaviour means that for some specific excitation energy there are several and at least two possible wavevectors. So for this excitation frequency, modes are necessarily complex. As a matter of fact for such rather low absolute values of the long distance coupling c , there is already a non monotonic behaviour of the dispersion relation of surface waves. This intriguing situation requires considering a few illustrative examples.

-3.d Let us consider now a specific case of interference between all ranges where all layers bring the same contribution ($a = b = c = d = \dots = 1$) to the interlayer coupling. This is the approximate case of pure dipolar interactions in many layered materials [23] as it can be easily checked from an integral estimation of the dipolar coupling. In that case the dispersion law (7) reads:

$$\begin{aligned}
 E &= 1 - 2 \cos(ka_0) - 2 \cos(2ka_0) - 2 \cos(3ka_0) - 2 \cos(4ka_0) - \dots \\
 &= 1 - \sum_{n=1}^N \left(\exp[ikna_0] + \exp[-ikna_0] \right)
 \end{aligned} \tag{10}$$

And after a geometric sum over the layer number, the more compact formula of the dispersion relation is obtained:

$$E = 1 - 2 \cos \left[\left(N + 1 \right) \frac{ka_0}{2} \right] \frac{\sin(Nka_0 / 2)}{\sin(ka_0 / 2)} \tag{10a}$$

Equations (10) and (10a) give for dispersion relation the diffraction pattern of a line of atoms parted by a distance a_0 between nearest atoms. So a cardinal sine is obtained. It explicitly underlines the non monotonic behaviour of the dispersion law as shown on Figure 2.

This classical result remembers us that for very low real values of the wavevector k , i.e. for large wavelength λ , there is a positive interference between all interacting layers, all terms add positively in equation (10), while for larger values of the wavevector, destructive interferences occur, and the

dispersion law can no longer be monotonic. Of course this remark has strong consequences upon the selection of stationary modes in thin films and especially in the case where dipolar coupling is not neglected, as just noticed from equations (10).

3.e In the more complex case of dipolar and exchange interactions, the effective dispersion law results from the superposition of equations (9) and (10) or (10a). So the shape of the dispersion law results from the addition of a parabola and a cardinal sine or of a sine function and a cardinal sine according to the relative intensities. In this case as well as in the previous case of a pure dipolar coupling, a non monotonic behaviour of the dispersion law appears and numerous excited modes involve several competing wavelengths.

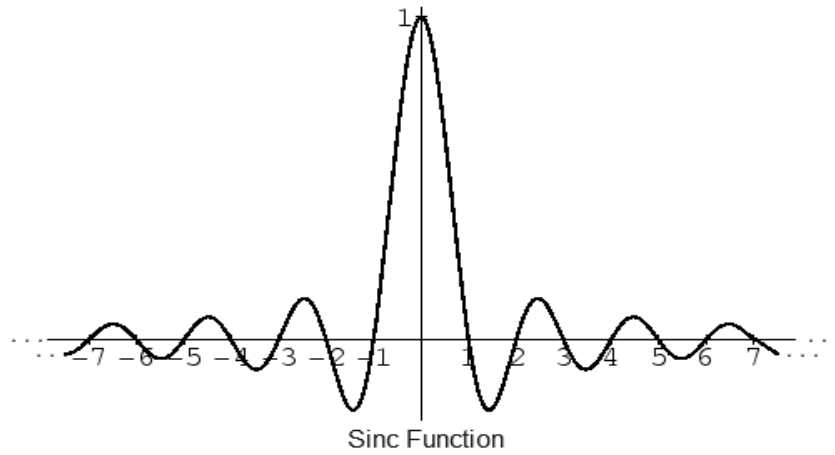


Figure 2. Cardinal sine is a weakly oscillating function.

4. Stationary modes in thin films

In order to find the stationary modes in a thin film, all equations of motion (6) must be considered together. Of course this requires the introduction of effective boundary conditions for the first and last layers. The complete resolution of this system of equations can be achieved in two ways. First there is the global method of dynamical matrix which consists in solving this matrix equation as a whole according to a Green's function approach [3, 8], i.e. a correlation function approach. This method has the advantage of introducing physically meaningful correlation functions but it generally leads to tedious calculations. So it ends practically with a numerical resolution. On the other side, equations of motion can be considered locally as evolution equations for an incident signal entering the sample, then propagating

through the sample and finally leaving an outgoing signal. This is the local transfer matrix approach [18-20]. Of course the local character of the transfer matrix is restricted by interaction range considerations. So when the interaction range is short, the transfer matrix approach enables us to find easily the eigen values and the eigen modes of stationary waves. This is a real advantage even for medium range interaction. For both pedagogical and practical purposes we will develop here the two methods for the search of stationary modes. And finally, we will use an elaborate matrix resolution [25] for dynamical matrix in the case of a finite range of interaction, and the results of this method are fruitfully compared to the results of the transfer matrix.

4. 1. Dynamical matrix approach of eigen modes

Let us put the linearized equations of motion (6) in a matrix form. This would require the explicit form of boundary conditions which are used in numerical approaches. Just focusing on the principles of the bulk resolution and on numerical results, we neglect surface contributions. So the dynamical matrix \mathbf{A} is deduced from the set of equations:

$$\begin{aligned}
 (a-E)u_n - b(u_{n+1} + u_{n-1}) - c(u_{n+2} + u_{n-2}) - d(u_{n+3} + u_{n-3}) + \dots &= 0 \\
 (a-E)u_{n+1} - b(u_{n+2} + u_n) - c(u_{n+3} + u_{n-1}) - d(u_{n+4} + u_{n-2}) + \dots &= 0 \\
 (a-E)u_{n+2} - b(u_{n+3} + u_{n+1}) - c(u_{n+4} + u_n) - d(u_{n+5} + u_{n-1}) + \dots &= 0 \\
 \dots &
 \end{aligned} \tag{11}$$

And so on. In a matrix form, it reads, here written in the case of 8x8 dynamical matrix \mathbf{A} :

$$\begin{pmatrix}
 a-E & -b & -c & -d & -e & . & . & . \\
 -b & a-E & -b & -c & -d & -e & . & . \\
 -c & -b & a-E & -b & -c & -d & -e & . \\
 -d & -c & -b & a-E & -b & -c & -d & -e \\
 -e & -d & -c & -b & a-E & -b & -c & -d \\
 . & -e & -d & -c & -b & a-E & -b & -c \\
 . & . & -e & -d & -c & -b & a-E & -b \\
 . & . & . & -e & -d & -c & -b & a-E
 \end{pmatrix}
 \begin{pmatrix}
 u_1 \\
 u_2 \\
 u_3 \\
 u_4 \\
 u_5 \\
 u_6 \\
 u_7 \\
 u_8
 \end{pmatrix}
 = \mathbf{A} * \mathbf{u} =
 \begin{pmatrix}
 0 \\
 0 \\
 0 \\
 0 \\
 0 \\
 0 \\
 0 \\
 0
 \end{pmatrix} \tag{11a}$$

So finally the eigen magnon frequencies are deduced from the resolution of the characteristic equation [3, 8, 14]:

$$\det \mathbf{A} = 0 \quad (12)$$

Of course including boundary conditions at the two external surfaces changes the dynamical matrix \mathbf{A} into an effective dynamical matrix $\mathbf{A}' = \mathbf{A} + \delta_1 + \delta_2$ where the correction matrices δ_1 and δ_2 have non zero elements only close to the first and last lines and columns respectively. These boundary corrections introduce surface and interface effects [3, 21].

The profiles of the eigen modes are deduced from the eigen vectors of the dynamical matrix \mathbf{A} or \mathbf{A}' as deduced from the equation on Green's function where the right term of equation (11a) is a delta function [3, 8]. This resolution practically requires inverting the dynamical matrix \mathbf{A} or \mathbf{A}' . As a matter of fact, if the inverse of \mathbf{A} is known, it is rather easy to find the inverse of \mathbf{A}' since $\mathbf{A}^{-1}\mathbf{A}'$ differs from the identity by a low rank matrix and this simple matrix can be easily inverted from elementary matrix operations [3, 26].

As previously done about dispersion relations, let us consider the same typical cases.

4.1.a. First the case of a very local coupling considered before ($b = c = d = \dots = 0$). Here the dynamical matrix is reduced to the main diagonal. Then all modes are degenerate up to surface conditions as defined from correction matrices. This degeneracy is well in agreement with the flat dispersion law.

4.1.b. Then let us consider the classical case of coupling with the two nearest layers ($a \neq 0, b \neq 0, c = d = \dots = 0$). This case was solved formally analytically in the case of surface effects restricted to a few layers, with evidence for possible surface modes according to boundary conditions given by the correction matrices [3, 26]. In that case all modes are perfectly sinusoidal, some of them with a pure imaginary wavevector – the surface modes –, the only specific point of these modes is the mode pinning at external surfaces which has been studied in different ways [27]. Figure 3 shows these regular profiles. This regularity has for consequence a regular variation of the intensity profile in spin wave resonance with line number according to a power law [4]. So the simple inspection of resonance lines evidences surface waves and pinning conditions at the surfaces [4].

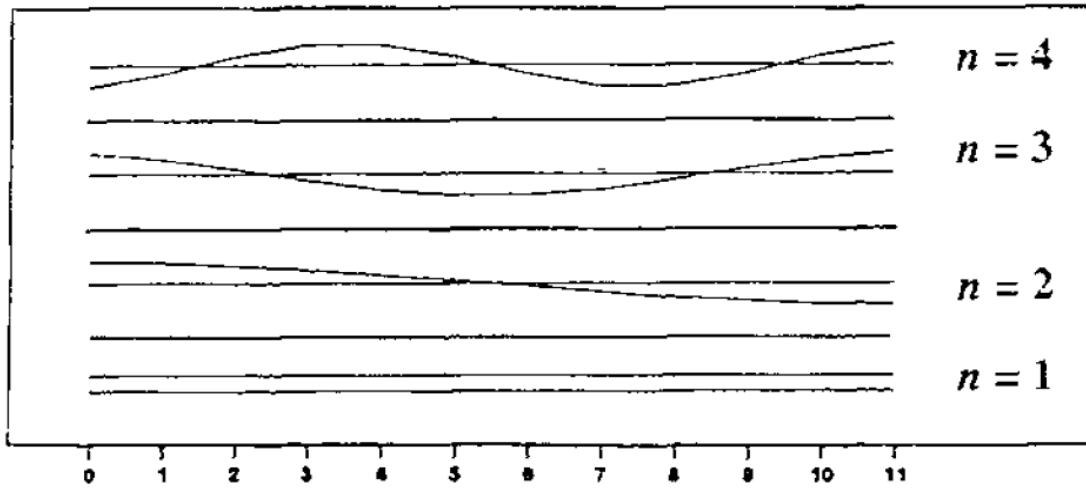


Figure 3. The numerical profiles of the four lowest lying eigenmodes of a finite chain of 12 atoms, with a constant nearest neighbour coupling only [23] are shown. Note the sine like regularity.

4.1. c. The case where two different layers are coupled: $c \neq 0$ in equation (6) is more complex than the previous ones as already noticed about dispersion law.

4.1.c.1 If $b=0$, this case reduces to the previous case of coupling with the nearest layer with a double interlayer distance. So solutions are perfectly sinusoidal.

4.1.c.2 If $b \neq 0$, from the point of view of dispersion relation (7) there are two competing wavevectors: k and $2k$. From numerical computations with given boundary conditions [23], the spin wave profile is also non sinusoidal as shown in Figure 4. Of course the mixing of these two contributions depends on boundary conditions, so exponential and sinusoidal functions can be mixed.

4.1.d Let us now consider the extreme case of interference between all ranges where all layers but the first give the same contribution ($b = c = d = \dots = 1$) to the spin deviation of the reference layer. This is the approximate case of pure dipolar interactions in many layered materials [23]. The dynamical matrix equation is reported here in the case of 8 layers, when neglecting boundary conditions, of course this number 8 is chosen for clarity.

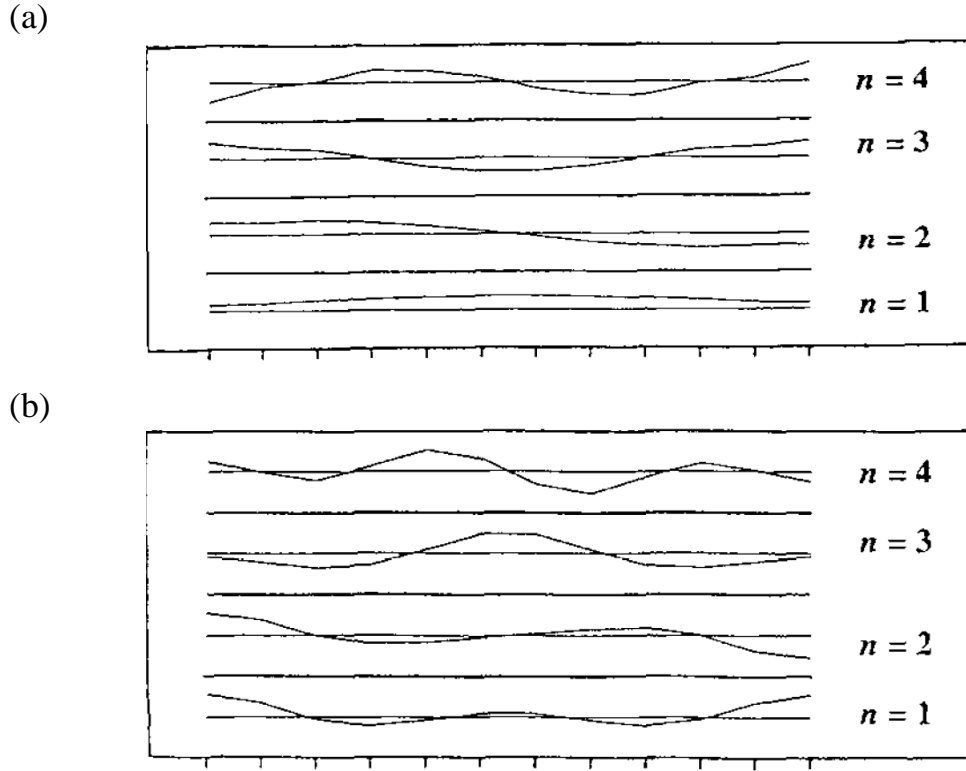


Figure 4. The numerical profiles of the four lowest lying eigenmodes of a finite chain of 12 atoms, with a constant nearest neighbour (NN) coupling and a constant next nearest neighbour (NNN) coupling[23]. In the upper part (a), the NNN coupling has the same sign as the NN coupling while in the lower part (b), the NNN coupling has the opposite sign. Note the complexity of these profiles as compared to those of Fig. 3.

$$\begin{pmatrix} a-E & -1 & -1 & -1 & -1 & -1 & -1 & -1 \\ -1 & a-E & -1 & -1 & -1 & -1 & -1 & -1 \\ -1 & -1 & a-E & -1 & -1 & -1 & -1 & -1 \\ -1 & -1 & -1 & a-E & -1 & -1 & -1 & -1 \\ -1 & -1 & -1 & -1 & a-E & -1 & -1 & -1 \\ -1 & -1 & -1 & -1 & -1 & a-E & -1 & -1 \\ -1 & -1 & -1 & -1 & -1 & -1 & a-E & -1 \\ -1 & -1 & -1 & -1 & -1 & -1 & -1 & a-E \end{pmatrix} = \mathbf{A} \quad (13)$$

From elementary matrix operations, only two different eigenvalues for this general case are found: $E = a - 1$ and $E = a + (N - 1)$ which is $(N - 1)$ times

degenerate. The first eigenvalue $E = a - 1$ corresponds to the uniform mode with all spin deviations equal. Comparing this result with the sine cardinal dispersion law (10a) previously obtained for such a material means that there is a long wavelength mode which is the uniform mode and that many degenerate modes are composed with several shorter wavelengths. More realistic cases can be dealt with by introducing perturbations of this ideal dynamical matrix. Such results show an obvious memory of this basic degeneracy. As a matter of fact the numerical resolution of such specific problems [24] gives a rather narrow band of modes instead of the degenerate modes and a well separated uniform mode as shown in Figure 5.

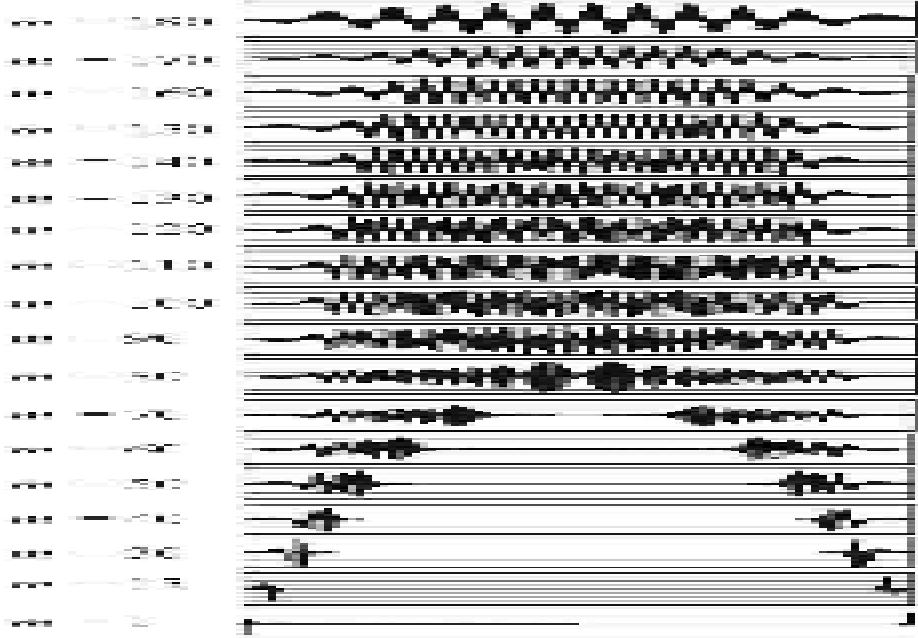


Figure 5. Numerically calculated mode profiles are shown with increasing frequency from the bottom to the top in a rod of length 200. The lowest mode is the mode number 1. The following mode numbers are, respectively, 15, 30, 40, 50, 60, 70, 80, and so on up to 180. All these modes are localized either close to the surfaces ($n < 80$) or near the centre of the rod ($80 < n < 180$) [24].

4. 2. Transfer matrix approach of spin wave modes

The transfer matrix approach of magnon modes consists in writing the one step evolution of a local set of spin deviations in order to introduce an iterative treatment. Practically, when the interaction range is restricted to N layers, the $2N$ independent equations of motion read:

$$\begin{aligned}
u_{n+N} &= -\frac{a_{N-1}}{a_N}u_{n+N-1} - \frac{a_{N-2}}{a_N}u_{n+N-2} - \dots + \frac{a_0 - E}{a_N}u_n - \dots - \frac{a_{N-2}}{a_N}u_{n-N+2} - \frac{a_{N-1}}{a_N}u_{n-N+1} - u_{n-N} \\
u_{n+N-1} &= u_{n+N-1} \\
&\dots \\
u_{n-N+1} &= u_{n-N+1}
\end{aligned} \tag{14}$$

Where the general numeric order 0,1,2,... of indices has been used instead of the alphabetic order: a, b, c, previously used, with obviously $b = a_1$, $c = a_2$, $d = a_2$, $e = a_3$,... and where the reticular distance a_0 between successive reticular planes cannot be confused with a coupling coefficient.

This set of 2N equations (14) read in a matrix form defines the local 2Nx2N transfer matrix **T** by the iteration equation:

$$\begin{pmatrix} u_{n+N} \\ u_{n+N-1} \\ \vdots \\ u_{n-N+2} \\ u_{n-N+1} \end{pmatrix} = \begin{pmatrix} -\frac{a_{N-1}}{a_N} & \frac{a_{N-2}}{a_N} & \cdot & \frac{a_{N-1}}{a_N} & -1 \\ 1 & 0 & 0 & 0 & 0 \\ \cdot & \cdot & \cdot & \cdot & \cdot \\ 0 & 0 & \cdot & 0 & 0 \\ 0 & 0 & 0 & 1 & 0 \end{pmatrix} * \begin{pmatrix} u_{n+N-1} \\ u_{n+N-2} \\ \vdots \\ u_{n-N+1} \\ u_{n-N} \end{pmatrix} \tag{15}$$

i.e. in a matrix notation:

$$\mathbf{u}_{n+N} = \mathbf{T} * \mathbf{u}_{n+N-1} \tag{16}$$

A simple calculation shows that this transfer matrix **T** is unitary as expected. The final transfer matrix equation includes the boundary conditions [18] and reads when magnetic parameters are the same throughout the sample:

$$P(\mathbf{T}) = 0 \tag{17}$$

Where $P(x)$ is a polynomial of the variable x . The polynomial order is the number of film layers.

Now the bulk transfer matrix diagonalization gives:

$$\mathbf{T} = \mathbf{MDM}^{-1} \tag{18}$$

Where **D** is a diagonal 2Nx2N matrix with N root pairs. These root pairs are either a complex root and its complex conjugate – in that case this defines a bulk wave- or a real root and its inverse – in that case this defines a surface

mode-. This pairing is due to the symmetric property of the transfer matrix \mathbf{T} for ingoing and outgoing waves. Matrix \mathbf{M} is a convenient unitary $2N \times 2N$ matrix.

From this diagonalization equation, the evolution equation (16) can be rewritten as:

$$\mathbf{u}_{n+N} = \mathbf{T}^{N+n} * \mathbf{u}_0 = \mathbf{M} \mathbf{D}^{N+n} \mathbf{M}^{-1} * \mathbf{u}_0 \quad (19)$$

Developing this equation shows that the eigen mode profiles result from the superposition of N surface waves and sinusoidal waves since because of symmetry the bulk transfer matrix has for eigen values s and s^{-1} or s^* for a complex value.

As done before, let us consider now a few typical cases of transfer matrices for the same magnetic interactions.

4.2.a. First the case of a very local coupling ($b = c = d = \dots = 0$). There is no need to define a transfer matrix. Then all modes are degenerate up to surface conditions.

4.2.b Then let us consider the classical case of coupling with the two nearest layers ($a \neq 0, b \neq 0, c = d = \dots = 0$). In that case the transfer matrix is 2×2 and reads:

$$= \begin{pmatrix} \frac{a-E}{b} & -1 \\ 1 & 0 \end{pmatrix} \quad (20)$$

The diagonalization of this transfer matrix gives the characteristic equation:

$$s^2 - \frac{a-E}{b}s + 1 = 0 \quad (21)$$

There are two conjugate eigenvalues:

$$s_{\pm} = \frac{a-E}{2b} \pm \sqrt{\left(\frac{a-E}{2b}\right)^2 - 1} \quad (22)$$

And according to equation (19) the mode profile is given by:

$$u_n = Cs_+^n + Ds_-^n \quad (23)$$

As introduced before, modes are so either surface modes or sinusoidal modes according to the reality or not of the values s_- and s_+ . This is due to the symmetry of equation (21). For a real value of s , the depth of penetration of the surface wave is: $|\ln s|^{-1}$. And for a unit complex number s , the wavevector

of this mode is $\arg(s)$ or $\arccos \frac{a-E}{2b}$. This proves the sinusoidal character

of such spin waves. This was expected from the monotonic behaviour of the dispersion relation but is not easy to demonstrate directly from the dynamical matrix with boundary conditions [3, 8, 26]. It was observed in the numerical computation of Fig. 3 [23].

4.2. c. The case where two different layers on each side are coupled: $c \neq 0$ in equation (6) defines as usual a transfer matrix which is here a 4x4 matrix:

$$\begin{pmatrix} u_{n+2} \\ u_{n+1} \\ u_n \\ u_{n-1} \end{pmatrix} = \begin{pmatrix} -\frac{b}{c} & \frac{a-E}{c} & -\frac{b}{c} & -1 \\ 1 & 0 & 0 & 0 \\ 0 & 1 & 0 & 0 \\ 0 & 0 & 1 & 0 \end{pmatrix} \begin{pmatrix} u_{n+1} \\ u_n \\ u_{n-1} \\ u_{n-2} \end{pmatrix}$$

It defines $T = \begin{pmatrix} -\frac{b}{c} & \frac{a-E}{c} & -\frac{b}{c} & -1 \\ 1 & 0 & 0 & 0 \\ 0 & 1 & 0 & 0 \\ 0 & 0 & 1 & 0 \end{pmatrix}$ (23)

Then the diagonalization of this transfer matrix gives a characteristic polynomial of degree four of the eigenvalue s :

$$s^4 + \frac{b}{c}s^3 - \frac{a-E}{c}s^2 + \frac{b}{c}s + 1 = 0 \quad (24)$$

Fortunately the previously noticed symmetry property of propagation associates the two ways of propagation: s and s^{-1} as before. So taking

advantage of this property, the new variable $u = s + s^{-1}$ is introduced. This substitution leads to a characteristic equation of second order in the variable u which is twice the wavevector of this mode in the case of a sinusoidal wave:

$$u^2 + \frac{b}{c}u - 2 - \frac{a-E}{c} = 0 \quad (25)$$

This equation is easily solved with the result for this reciprocal function of the eigenvalues:

$$u_{\pm} = -\frac{b}{2c} \pm \sqrt{\frac{b^2}{4c^2} + 2 + \frac{a-E}{c}}$$

Then the four eigenvalues s_1, s_2, s_3, s_4 are deduced from u_{\pm} .

Finally in the case of two sinusoidal waves the mode profile deduced from equation (19) reads:

$$u_n = C_1 s_1^n + C_2 s_2^n + C_3 s_3^n + C_4 s_4^n \quad (26)$$

So this real mode is calculated for a given frequency or energy E and looks like the combination of two sinusoidal or surface waves since the s_1, s_2, s_3, s_4 eigenvalues are working by pairs linked with u_- and u_+ , in perfect agreement with the result reported in Figure 4, from numerical results deduced from the dynamical matrix resolution [23].

$$u_{\pm} = 2 \cos \mathcal{G}_{\pm} \quad \text{and}$$

$$u_n = C_+ \cos(n\theta_+ - \phi_+) + C_- \cos(n\theta_- - \phi_-) \quad (27)$$

Of course there is an agreement between the two last paragraphs when b is equal to zero. In that case $u_{\pm} = -u_{\mp}$ and so $\mathcal{G}_{\pm} = \mathcal{G}_{\mp} + \pi \ (2\pi)$. So the two waves cannot be distinguished since the nearest coupled layer is the second one! This can also be deduced from the comparison between equations (21) and (25).

4.2. d. Let us consider the new intermediate case when p layers on each side are coupled to the layer n ($a_q = 0$, when $q > p$). Then the equation of motion (6) defines a $(2p) \times (2p)$ transfer matrix:

$$\mathbf{T} = \begin{pmatrix} -\frac{a_{p-1}}{a_p} & \cdot & \frac{a_0 - E}{a_p} & \cdot & -\frac{a_{p-1}}{a_p} & -1 \\ 1 & 0 & 0 & 0 & 0 & 0 \\ 0 & 1 & 0 & 0 & 0 & 0 \\ 0 & 0 & 1 & 0 & 0 & 0 \\ 0 & 0 & 0 & 1 & 0 & 0 \\ 0 & 0 & 0 & 0 & 1 & 0 \end{pmatrix} \quad (28)$$

Where the generalization of this transfer matrix which has a first line of non zero elements as defined from equation (14) and a lower diagonal of unit value to any order p is quite obvious.

As noticed before the general diagonalization of this transfer matrix leads to a characteristic equation of order $2p$ in the eigenvalue s . And the previously noticed symmetry property of propagation associates the two ways of propagation: s and s^{-1} . So taking advantage of this property, the new variable $u = s + s^{-1}$ is introduced with as a consequence the appearance of a characteristic polynomial equation of order p in the symmetric variable u .

$$P_p(u) = 0 \quad (29)$$

Now the resolution of this new characteristic equation gives p pairs of solutions s and s^{-1} . Back to the transfer matrix it means that mode profiles result from the linear combination of p sinusoidal, i.e. bulk, or exponential, i.e. surface, waves. This result is quite in agreement with the dispersion law where frequency results from a sum of p terms of different wavevectors. This result is also in agreement with the observation of Figure 5 where eigen modes are quite complex in the considered case of dipolar interaction, i.e. when p is very large, as large as the layer number.

4.2. e. In the case of dipolar interactions where all layers are coupled, the extension of the previous result confirms the complexity of eigen modes which are linear combinations of many sinusoidal parts. Then the transfer matrix approach is not really simpler than the dynamical matrix approach, even if the transfer matrix contains more zeroes than the dynamical matrix and so is more easily computed.

4.3. Analytical approach of the dynamical matrix

One serious improvement in the theory of dynamical matrix comes from the use of simple matrix polynomials for considering dynamical matrix. It

consists in taking advantage of the dynamical matrix symmetry properties, a mirror property according to the first diagonal, and a translational invariance for a shift parallel to the first diagonal. So a simple generic matrix δ made of unit matrix elements for $(n, n+1)$ and $(n+1, n)$ for all valid positions and of zeroes in other places is easily proposed as a basic matrix fulfilling these symmetry properties:

$$\delta = \begin{pmatrix} 0 & 1 & 0 & 0 & 0 & 0 & 0 & 0 \\ 1 & 0 & 1 & 0 & 0 & 0 & 0 & 0 \\ 0 & 1 & 0 & 1 & 0 & 0 & 0 & 0 \\ 0 & 0 & 1 & 0 & 1 & 0 & 0 & 0 \\ 0 & 0 & 0 & 1 & 0 & 1 & 0 & 0 \\ 0 & 0 & 0 & 0 & 1 & 0 & 1 & 0 \\ 0 & 0 & 0 & 0 & 0 & 1 & 0 & 1 \\ 0 & 0 & 0 & 0 & 0 & 0 & 1 & 0 \end{pmatrix} \quad (30)$$

Here a 8x8 matrix is shown and the generalization to any size is obvious. Then it is easy to show that even and odd powers of this matrix are, also made of diagonals with the required symmetry properties, up to “surface” terms at their boundaries which are here neglected.

These odd and even matrices are:

$$\delta^{2p+1} = \begin{pmatrix} 0 & . & 0 & . & 0 & . & 0 & . \\ . & 0 & . & 0 & . & 0 & . & 0 \\ 0 & . & 0 & . & 0 & . & 0 & . \\ . & 0 & . & 0 & . & 0 & . & 0 \\ 0 & C_{2p+1}^{p-1} & 0 & C_{2p+1}^p & 0 & C_{2p+1}^{p+1} & 0 & C_{2p+1}^{p+3} \\ . & 0 & . & 0 & . & 0 & . & 0 \\ 0 & . & 0 & . & 0 & . & 0 & . \\ . & 0 & . & 0 & . & 0 & . & 0 \end{pmatrix}$$

$$\delta^{2p} = \begin{pmatrix} \cdot & 0 & \cdot & 0 & \cdot & 0 & \cdot & 0 \\ 0 & \cdot & 0 & \cdot & 0 & \cdot & 0 & \\ \cdot & 0 & \cdot & 0 & \cdot & 0 & \cdot & 0 \\ 0 & \cdot & 0 & \cdot & 0 & \cdot & 0 & \cdot \\ C_{2p}^{p-2} & 0 & C_{2p}^{p-1} & 0 & C_{2p}^p & 0 & C_{2p}^{p+1} & 0 \\ 0 & \cdot & 0 & \cdot & 0 & \cdot & 0 & \cdot \\ \cdot & 0 & \cdot & 0 & \cdot & 0 & \cdot & 0 \\ 0 & \cdot & 0 & \cdot & 0 & \cdot & 0 & \cdot \end{pmatrix} \quad (31)$$

Here just one central line of each matrix is shown as well as some diagonals of zeroes. The proof of this structure comes from the well known relation of combinatorial analysis [28]:

$$C_n^k + C_n^{k+1} = C_{n+1}^{k+1} \quad (32)$$

Evidence of the corrective surface terms to be included is clear from the observation of the first powers of this matrix δ where only the first lines and columns are shown for evidencing these progressively extended corrective surface terms:

$$\delta^2 = \begin{pmatrix} 1 & 0 & 1 & 0 & \cdot \\ 0 & 2 & 0 & 1 & \cdot \\ 1 & 0 & 2 & 0 & \cdot \\ 0 & 1 & 0 & 2 & \cdot \\ \cdot & \cdot & \cdot & \cdot & \cdot \end{pmatrix} \quad (33a)$$

$$\delta^3 = \begin{pmatrix} 0 & 2 & 0 & 1 & \cdot \\ 2 & 0 & 3 & 0 & \cdot \\ 0 & 3 & 0 & 3 & \cdot \\ 1 & 0 & 3 & 0 & \cdot \\ \cdot & \cdot & \cdot & \cdot & \cdot \end{pmatrix} \quad (33b)$$

$$\delta^4 = \begin{pmatrix} 2 & 0 & 3 & 0 & 1 & . \\ 0 & 5 & 0 & 4 & 0 & . \\ 3 & 0 & 6 & 0 & 4 & . \\ 0 & 4 & 0 & 6 & 0 & . \\ 1 & 0 & 4 & 0 & 6 & . \\ . & . & . & . & . & . \end{pmatrix} \quad (33c)$$

$$\delta^5 = \begin{pmatrix} 0 & 5 & 0 & 4 & 0 & 1 & . \\ 5 & 0 & 9 & 0 & 5 & 0 & . \\ 0 & 9 & 0 & 10 & 0 & 5 & . \\ 4 & 0 & 10 & 0 & 10 & 0 & . \\ 0 & 5 & 0 & 10 & 0 & 10 & . \\ 1 & 0 & 5 & 0 & 10 & 0 & . \\ . & . & . & . & . & . & . \end{pmatrix} \quad (33d)$$

Quite obviously the surface correction order increases with the matrix power. So finally each dynamical matrix can be written as a sum of powers of that matrix δ multiplied by convenient real coefficients with the identity matrix times a convenient real coefficient. The dynamical matrix is a real polynomial of this matrix δ , up to corrective surface terms.

$$\mathbf{A} = P(\delta, \mathbf{I}) \quad (34)$$

As noticed before, these surface corrections can be dealt with later. So since all these power matrices commute together, standard algebraic operations on complex numbers are valid for this matrix polynomial \mathbf{A} . So this polynomial expression can be factorized, when using its complex roots:

$$\mathbf{A} = P(\delta, \mathbf{I}) = C \prod_i (\delta - s_i \mathbf{I}) \quad (35)$$

So the dynamical matrix is easily inverted by means of standard operations:

$$\mathbf{A}^{-1} = \sum_i C_i (\delta - s_i \mathbf{I})^{-1} \quad (36)$$

In equation (36) the coefficients C_i are deduced from the factorization of the rational fraction $P(\delta, \mathbf{I})$ into simple elements. The matrix elements of $(\delta - s_i \mathbf{I})^{-1}$ are known to be sine functions for real wavevectors, i.e. unitary values of the roots s_i , from reference [26], appendix 2. Finally the eigen modes are deduced by taking into account the boundary conditions expressed by the surface matrices δ_1 and δ_2 . So the mode profiles result from a sum of sine functions of different wavevectors deduced from the s_i 's. This is the third demonstration of this result, after that of the dispersion law and that of transfer matrix. And these demonstrations are well in agreement with numerical observations of Figs. 4 and 5.

5. Conclusions

As a complement to these deductions let us recall some recent typical results of accurate observations of magnetic modes. Many observations of quite localized magnon modes, so well in agreement with the present analytic and numerical results, have been made in quite small samples and with high accuracy by means of different techniques in nonellipsoidal micrometer size magnetic elements [29]. Brillouin light scattering were also performed with various object shapes, always with evidence for localized modes, in micrometer permalloy wires [30], in nanometric elliptical dots arrays [31], on cylindrical permalloy dots [32], in rectangular dots [33] and in nanoelements [34]. Of course there is a basic agreement between these observations of localized modes and the present calculations. However there could be also other causes for such localization properties. For instance some of these samples were not magnetically saturated which implies a complex structure made of magnetic domains and such a structure could also force localization. The first diagonal part of the dynamical matrix is not uniform since the static demagnetizing field is not uniform throughout the sample [35]. This could be another cause of localization. Finally the present model is a one dimensional model and so neglects the three dimensional effect which induces a more complex variation near the external surfaces, with a more restricted meaning of localization. So these different effects also contribute to localization.

Numerous simulations using micromagnetism codes have been recently done, in various ways, and they share evidence for many localized modes and for a complex structure of modes [36-38]. This is also a strong proof for localization effects as well as for complex modes.

So both recent experimental observations and recent numerical work confirm this tendency towards non sinusoidal modes which appears in these calculations in the case of an extended coupling. This agreement favours a

short review of our different demonstrations of the complexity of magnon profiles in presence of a rather extended magnetic coupling;

- A first evidence for an influence of the interaction range comes from the dispersion law of progressive waves. Numerous cases of non monotonic dispersion laws are shown, and they favour a mode complexity.

- A direct evidence for mode complexity comes from the numerical resolution of the dynamical matrix. And this observed mode complexity is not the same for all modes. Some modes well deserve the name of uniform mode or of bulk modes while many new modes have peculiar localization properties..

- The transfer matrix approach for medium range interaction well shows the progressive increase of mode complexity with increasing interaction range.

- Finally the consideration of matrix algebra enables us to recover analytically the stationary mode complexity directly from the dynamical matrix in a rather simple way and in agreement with transfer matrix theory.

As last remarks, it must be said that the extension of this work to acoustical properties as well as to electronic properties sounds full of promise. For instance several recent works noticed the effects of phonon localization in presence of long range interactions as electric fields [39,40]. Of course the competition between long range interaction and finite sample size can be another cause of localization [41].

6. References

1. F. Bloch, Z. Physik **61**, 206 (1930).
2. C. Kittel, *Introduction to Solid State Physics*, 7th edition, Wiley, New York (1995).
3. J.-C.S. Levy, Surf. Sci. Rep. **1**, 39 (1980).
4. C. Kittel, Phys. Rev. **110**, 1295 (1958).
5. G. Rado and H. Suhl, “*Magnetism*” - Academic press (1963-1965-1966).
6. L. Pauling, Proc. Nat. Acad. Sci. **14**, 359 (1928).
7. W. H. Meiklejohn and C. P. Bean, Phys. Rev. **105**, 904 (1957)
8. S.V.Tyablikov, “*Methods in the Quantum Theory of Magnetism*” Plenum Press, New York, (1967); J.-C.S. Levy, E. Ilisca and J.-L. Motchane, Phys. Rev. B **5**, 187 (1972) and 1099 (1972).
9. L. Landau and E. Lifshitz, “*The classical Theory of Fields*” 2nd edition, Pergamon Press, London 118 (1962).
10. J. Villain, J. Phys. C **10**, 1717 (1977); G. Toulouse, Commun. Phys. **2**, 115 (1977).
11. T. Holstein and H. Primakoff, Phys. Rev. **58**, 1098 (1940); L.R. Walker, Phys. Rev; **105**, 390 (1957); R.W. Damon and J.R. Eshbach, J. Phys. Chem. Solids **19**, 308 (1961).
12. M.E. Fisher and W. Selke, Phys. Rev. Lett. **44**, 1502 (1980); W. Selke, Physics Reports **170**, 213 (1988).

13. See for instance “*Nanomagnetism*” edited by D.L. Mills and J.A.C. Bland, Elsevier, Amsterdam (2006).
14. E.Y. Vedmedenko “*Competing Interactions and Patterns in Nanoworld*” edited by Wiley-VCH Berlin (2007).
15. A. A. Maradudin, “*Solid State Physics*” (F. Seitz and D. Turnbull, editors, Academic Press 1966), **18**, **19**.
16. T. Toyama and S. Maekawa, Phys. Rev. B **49**, 3596 (1988).
17. E. W. Montroll, G. H. Weiss, J. Math. Phys. **6**, 167-181 (1965); N. W. Ashcroft, N. D. Mermin, *Solid State Physics*, ed. Holt, New York (1976).
18. J.-C.S. Levy, Phys. Rev. B **25**, 2893 (1982); D. Mercier, J.-C.S. Levy, M.L. Watson, J.S.S. Whiting and A. Chambers, Phys. Rev. B **43**, 3311 (1990); D. Mercier and J.-C.S. Levy, J. Mag. & Mag. Mat. **93**, 557 (1991).
19. D.M. Pozar, “*Microwave Engineering*”, 3rd Edition. John Wiley & Sons, New York (2005).
20. H. Poincaré, Acta Math. **13**, 1 (1890).
21. H. Puszkarski, Progress in Surface Science **9**, 191 (1979); **25**, 155 (1987).
22. S. Mamica and H. Puszkarski, in “*Surface Magnetism and Nanostructures*” eds. A. Ghazali and J.-C.S. Levy, Research Signpost, Trivandrum, India, 129 (2006).
23. H. Puszkarski, J.-C.S. Levy and D. Mercier, Phys. Lett. A **232**, 275 (1997).
24. H. Puszkarski, M. Krawczyk and J.-C.S. Levy, Phys. Rev. B **71**, 14421 (2005); phys. stat. sol. (b) **243**, 65 (2006) ; J. Appl. Phys. **101**, 02436 (2007).
25. J.-C.S. Lévy, D. Mercier, H. Puszkarski and M. Krawczyk, Recent Res. Devel. Magnetism & Magnetic Mat. **2**, 1 (2004).
26. J.-C.S. Levy, E. Gallais and J.-L. Motchane, J. Phys. C **7**, 761, (1974).
27. M. Sparks, Phys. Rev. B **1**, 3831, 3856, 4439 (1970); H. Puszkarski, Progr. Surf. Sci., **9**, 109 (1979), Surf. Sci. Rep. **20**, 45 (1994).
28. W. Feller, “*An introduction to probability and its applications*”, J. Wiley and sons, New York (1957).
29. J. Jorzick, S.O. Demokritov, B. Hillebrands, M. Bailleul, C. Fermon, K.Y. Guslienko, A.N. Slavin, O.V. Berkov and N.L. Gorn, Phys. Rev. Lett. **88**, 47204 (2002); J.P. Park, P. Eames, D.M. Berezovsky and P.A. Crowell, Phys. Rev. Lett. **89**, 277201 (2002).
30. Y. Roussigné, S.M. Chérif, C. Dugautier and P. Moch, Phys. Rev. B **63**, 134429 (2002).
31. G. Gubbioti, O. Kazakova, G. Carlotti, M. Hanson and P. Vassavori, IEEE Trans. Magn. **39**, 2750 (2003).
32. G. Gubbioti, G. Carlotti, R. Zivieri, F. Nizzoli, T. Okuno and T. Shinjo, J. Appl. Phys. **93**, 7607 (2003); G. Gubbioti, G. Carlotti, T. Okuno, T. Shinjo, F. Nizzoli and R. Zivieri, Phys. Rev. B **68**, 184409 (2003).
33. G. Gubbioti, M. Conti, G. Carlotti, P. Candeloro, E. Di Fabrizio, K.Y. Guslienko, A. Andre, C. Bayer and A. N. Slavin, J. Phys.: Condens. Matter **16**, 7709 (2004).
34. V.V. Kruglyak, P.S. Keatley, R.J. Hicken, J.R. Childress and J.A. Katine, J. Appl. Phys. **97**, 10A706 (2005).
35. H.J.G. Draaisma and W.J.M. De Jonge, J. Appl. Phys. **64**, 3610 (1988).
36. R.D. McMichael and M.D. Stiles, J. Appl. Phys. **97**, 10J901 (2005).

37. V.V. Kruglyak, P.S. Keatley, R.J. Hicken, J.R. Childress and J.A. Katine, J. Appl. Phys. **99**, 08F306 (2006).
38. Ph. Depondt and F.G. Mertens, preprint.
39. S. Kalliakos, P. Lefebvre, X.B. Zhang, T. Talercio, B. Gil, N. Grandjean, B. Damilano and J. Massies, phys. stat. sol. (a) **190**, 149 (2002).
40. S.G. Cloutier, C.-H. Hsu, P.A. Kossyrev and J. Xu, Adv. Mater. **18**, 841 (2006).
41. T.-R. Yang, M.M. Dvoynenko and H.H. Cheng, Physica B **329-333**, 1302 (2003).